1990

Time domain finite difference method for 3-D transmission line structures

Zhigang Ma
Lehigh University

Time Domain Finite Difference Method for 3-D Transmission Line Structures

by

Zhigang Ma

A Thesis
presented to the Graduate Committee
of Lehigh University
in candidacy for the degree of
Master of Science in Electrical Engineering

Lehigh University
Bethlehem, Pennsylvania
1989, 9

This thesis is accepted and approved in partial fulfillment of the requirements for the degree of Master of Science in Electrical Engineering.

Sept. 18, 1989
Date:

D. R. Decker
Dr. D. R. Decker
Advisor in Charge

L J Varnerin
Dr. L. J. Varnerin
CSEE Department Chairperson

ACKNOWLEDGEMENTS

I would like to acknowledge with deepest gratitude the valuable guidance, suggestions, encouragement and great detail help in C language programming provided by my thesis advisor Prof. R. Decker. I would also like thank both Dr. Olson and Mr. Ed Li for providing enlightening suggestions. Finally I wish especially to thank my wife Shexin Gong for her assistance in many ways.

The work reported here was supported by grants from GE and IBM.

TABLE OF CONTENTS

List of Figures

ABSTRACT

Time Domain Finite Difference Method for 3-D Transmission Line Structures

Time domain computation of electromagnetic fields is becoming a practical technique because of the availability of high speed and large memory computers. The time domain finite difference method and its supporting theories are presented. A strip-line with plated through hole (PTH) structure as an example of a 3-D transmission line has been investegated and numerical results of the propagation of a Gaussian pulse are presented in time sequence.

1. INTRODUCTION

Since the 1970s, an important shift has taken place in the design of computer hardware with the advent of smaller and denser integrated circuits and packages. Previously, the hardware components consisted of both physically and electrically large discrete components. Stray elements and coupling among the components were small in most cases and the interconnections between the components were electrically insignificant. The corresponding electrical network models were highly decoupled and the network analysis matrices sparse. This led to relatively simple analysis models and techniques for the electrical performance of these systems.

In contrast, today's high level of integration can lead to very large and complex systems with extremely small physical dimensions. An electrical analysis which excludes coupling among the closely spaced components is invalid. Further , the interconnections such as 3-D transmission line, which once led to insignificant stray elements are now the main elements in the equivalent circuit. Thus , the circuit models for integrated circuit systems are extremely complex, with highly coupled components. An electrical analysis of these models without computer-aided computation is impossible, especially for high performance systems.

1.1 Methods Avaliable for Modelling Transmission Line Discontinuities

1.1.1 Mode Matching Method

The study of Transmision line discontinuities has more than two decades of history. For nearly a decade , the analyses were mostly quasi-static in nature. The first accurate full-wave frequency-dependent analysis appeared around 1975 [1] [2]. This approach began with the use of a waveguide model with electric-wall top and bottom planes and magnetic-wall side planes to characterize the microstrip. The effective dielectric constant of the filling and the width of the guide are assumed to be frequency dependent and are determined in such a way that the model and the actual microstrip line have the same frequency dependent propagation coefficient and characteristic impedance. Using the waveguide model to represent the original microstrip , the field in the region of the discontinuities are expanded into waveguide modes, and the modes of different regions are matched at the intersection planes. From the matching coefficients, the S matrix for different propagation modes can be calculated. The waveguide model approach is efficient and has reasonable accuracy for calculating the magnitude of the S parameters in the lower frequency range, but it is not able to take into account radiation effects and surface wave generation . Beside , the mode-matching step will also introduce error due to the fact that the actual modes excited in microstrip discontinuities are not the same as those used in the model and accordingly will not match in exactly the same way. There is also an obvious limitation on the kinds of structures to which this method can be applied. It cannot , for example , be used to analyze the microstrip open-end structure where one side of the discontinuity is not connected to a microstrip and where radiation and surface waves are present.

1.1.2 Full Wave Approach

A full-wave approach to the microstrip open end problem was first proposed by James and Henderson [3]. The analysis on the microstrip open end , where the surface wave and radiation wave are the constitutents of the fields, is carried out using an analytic mode-expansion technique. On the microstrip side, a TEM wave is taken as the dominant mode incident field , and the semiempirical results for the propagation coefficient and the characteristic impedance are used for this incident wave . The fields at both sides are matched at the interface and a variational step is taken to reduce the error introduced by the assumption of a TEM field pattern where the electric field has a constant vertical value under the strip and is zero elsewhere in the transverse plane. Mainly due to the roughness of the field pattern assumed, the results of this method are not very accurate, but the analysis did provide valuable physical insight.

1.1.3 Spectral Domain Approch

Another important method which has been used by several investigators to model microstrip discontinuities is the spectral-domain approach[4]. In using this method to analyze shielded or covered structures, the fields and currents involved are Fourier transformed into the so called spectral-domain. The shape of the current on the microstrip is assumed to be close to actual current distribution and is easily Fourier-transformable. The spectral-domain components of the fields and currents are related according to the field continuity and boundary conditions and thus establish a system of equations for the variables. The inverse-transformed field solutions are used to calculate the S parameters.

Although it is a relatively accurate method for the type of components it is capable of calculating, the spectral-domain approach depends strongly on the current distributions assumed, which in many cases are hard to specify with high accuracy; thus it is limited due to the difficulties which arise near the cutoff frequency of the higher order mode of the microstrip.

1.1.4 Moment Method

In recent years, the moment method has also been used [5], [6] on discontinuity problems. This method can in principle be accurate with wide applications, but due to the complexity of the Green's functions for the microstrip configration it is not economical to make a very fine division of the microstrip for accurate results. In fact, in many cases only a rational function form is used on the microstrip , which may not correspond to the actual current distribution .

1.1.5 Time Domain Approach

All the above-mentioned investigations are done in the frequency domain; that is , the data for the whole frequency range are calculated one frequency at a time. It is an expensive task when the results of a wide frequency range are sought. This led us to seek an alternative way of calculating the frequency domain data. Since a pulse response contains all the information of a system for the whole frequency range, it is a natural approach to use a pulse in the time domain to excite the microstrip structures and from the time domain pulse response to extract the frequency domain characteristics of the system via the Fourier transform [7].

One numerical scheme which can be used to calculate the time domain fields is the Time Domain Finite Difference (TDFD) method introduced by K.S. Yee in 1966 [8] that has been used by many invesgators to solve electromagnetic scattering problems. Other numerical methods which can also be used to solve this type of initial boundary value problem include the TLM method and Bergeron's method. Among these methods the TDFD method is the most direct from a mathematical point of view. Some investigators found that the TDFD method is especially suitable for the accurate calculation of the microstrip field [9] .

1.2 TDFD Approach and Its Development

What is TDFD? This idea is as old as Confucius, who said : " From the knowledge of one corner, he (a good student) finds those of the other three, By studying the past, he (a good teacher) predicts the future."
(Paraphrased from Analecta of Confucius)

1.2.1 Yee's Idea

The Time-Domain Finite Difference Method was first introduced by K. S. Yee. In general, solutions to the time-dependent Maxwell's equations are unknown except for a few special cases. The difficulty is due mainly to the imposition of the boundary conditions. Yee proposed a method to obtain the solution numerically when the boundary conditions are those appropriate for a perfect conductor. This numerical method is employed for the most general case in theory. However the limited memory capacity of computers makes it impratical for very large dimension problems .

Maxwell's equations in an isotropic medium are :

$$\frac{\partial B}{\partial t} + \nabla\times E = 0 \qquad (1.1a)$$

$$\frac{\partial D}{\partial t} - \nabla \times H = J \qquad (1.1b)$$

$$B = \mu H \qquad (1.1c)$$

$$D = \epsilon E \qquad (1.1d)$$

where J , μ and ϵ are assumed to be given functions of space and time.

In a rectangular coordinate system, (1.1a) and (1.1b) are the following equations:

$$-\frac{\partial B_x}{\partial t} = \frac{\partial E_z}{\partial y} - \frac{\partial E_y}{\partial z} , \qquad (1.2a)$$

$$-\frac{\partial B_y}{\partial t} = \frac{\partial E_x}{\partial z} - \frac{\partial E_z}{\partial x} , \qquad (1.2b)$$

$$-\frac{\partial B_z}{\partial t} = \frac{\partial E_x}{\partial y} - \frac{\partial E_y}{\partial x} , \qquad (1.2c)$$

$$\frac{\partial D_x}{\partial t} = \frac{\partial H_z}{\partial y} - \frac{\partial H_y}{\partial z} - J_x , \qquad (1.2d)$$

$$\frac{\partial D_y}{\partial t} = \frac{\partial H_x}{\partial z} - \frac{\partial H_z}{\partial x} - J_y \qquad (1.2e)$$

$$\frac{\partial D_z}{\partial t} = \frac{\partial H_y}{\partial x} - \frac{\partial H_x}{\partial y} - J_z \qquad (1.2f)$$

To simulate wave propagation in three dimensions, Yee arranged the spatial points, where different components of E and H are to be calculated as in fig.1. The repetitive arrangement of the cells of fig.1 fills the computation domain with a finite difference mesh. Every component of H can be obtained by the loop integral of E using the four surrounding E nodal values according to Maxwell's equation for E. A similar approach holds for the calculation of H.

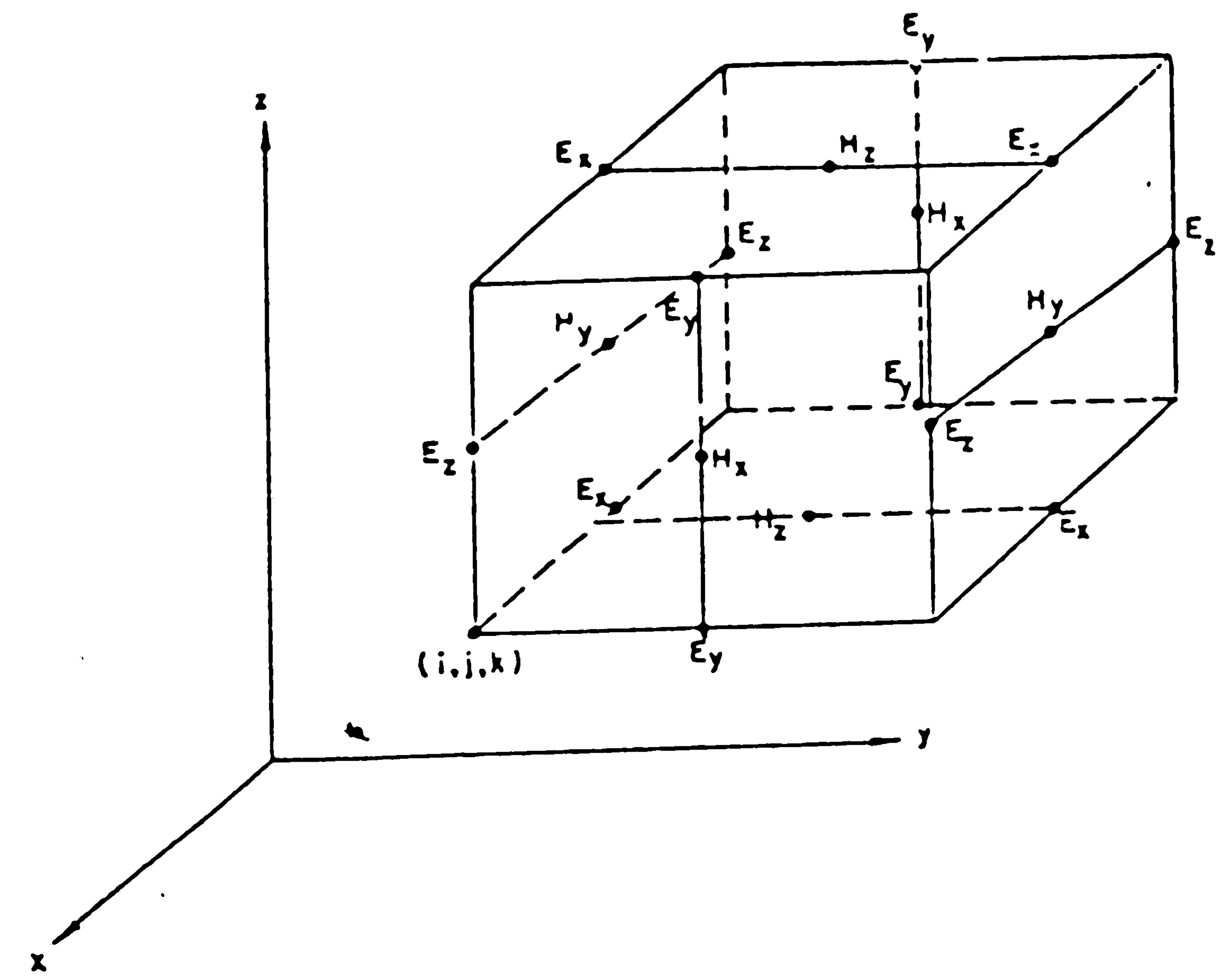

Fig. 1. Yee's grid

In this algorithm, not only the placement of the E and H nodes are off in space by half a space step, but the time instants when the E or H fields are calculated are also off by half a time step. To be more specific, if the components of E are calculated at $n\Delta t$, where Δt is the discretization unit in time, or the time step, and n is any nonnegative integer, the components of H are calculated at $(n + \frac{1}{2}) \Delta t$. For this reson , this algorithm is also called the leapfrog method.

A set of finite difference equations for (1.2a) - (1.2f) will be found if we denote a grid point of space as

$$(i, j, k) =(i\Delta x, j\Delta y, k\Delta z) \tag{1.3}$$

and for any function of space and time We put

$$F(i\Delta x, j\Delta y, k\Delta z, n\Delta t) = F^n(i, j, k) \qquad (1.4)$$

then for (1.2a) we have

$$\frac{B_x^{n+1/2}(i, j+\frac{1}{2}, k+\frac{1}{2}) - B_x^{n-1/2}(i, j+\frac{1}{2}, k+\frac{1}{2})}{\Delta t} = \frac{E_y^n(i, j+\frac{1}{2}, k+1) - E_y^n(i, j+\frac{1}{2}, k)}{\Delta z}$$

$$- \frac{E_z^n(i, j+1, k+\frac{1}{2}) - E_z^n(i, j, k+\frac{1}{2})}{\Delta y}. \qquad (1.5a)$$

$$\frac{D_z^n(i+\frac{1}{2}, j, k) - D_z^{n-1}(i+\frac{1}{2}, j, k)}{\Delta t}$$

$$= \frac{H_z^{n-1/2}(i+\frac{1}{2}, j+\frac{1}{2}, k) - H_z^{n-1/2}(i+\frac{1}{2}, j - \frac{1}{2}, k)}{\Delta y}$$

$$- \frac{H_y^{n-1/2}(i+\frac{1}{2}, j+\frac{1}{2}, k) - H_y^{n-1/2}(i+\frac{1}{2}, j - \frac{1}{2}, k)}{\Delta z} + J_x^{n-1/2}(i+\frac{1}{2}, j, k).$$

(1.5b)

The boundary conditions appropriate for a perfect conducting surface are that the tangential component of the electric field vanish and the normal component of the magnetic field vanish. The conducting surface will be approximated by a collection of surfaces of cubes, the sides of which are parallel to coordinate axes. For example, plane surfaces perpendicular to the x-axis will be chosen so as to obtain points where E_y and E_z are defined.

To have meaningful results by this method, the linear dimension of the grid must be only a fraction of the wavelengh. For computational stability, it is necessary to satisfy a relation between the space increment and time increment. When ϵ and μ are variables a rigorous stability criterion is difficult to obtain. For constant values of ϵ and μ computional stability requires that

$$\sqrt{(\Delta x)^2 + (\Delta y)^2 + (\Delta z)^2} > c\Delta t = \sqrt{\frac{1}{\epsilon\mu}}\ \Delta t \qquad (1.6)$$

where c is the velocity of light.

1.2.2 Yoshida, Fukai and Fukuoka Proposed Method

N. Yoshida, I. Fukai and J. Fukuoka proposed a numerical method for transient analysis in three dimensional space [10]. The method was based on the equations obtained by Bergeron [11] . The equations show the propagation of electromagnetic waves in an equivalent circuit based on Maxwell's equation. This method has two important advantages for the analysis. One is the formulation of the electromagnetic fields in terms of the variables in the equivalent circuits. This treatment enables us to see that the nodal equation is uniquely formulated in the equivlant circuit for both the electric field and the magnetic field because of the duality of both field components. The other advantage is the formulation by Bergeron's method with its many merits, such as the representation of the medium by the lumped elements at each node and its reactive characteristics which are represented by the trapezoidal rule of the differential equation in the time domain. This treatment is based on an iterative computation in time using only the values obtained after the previous step. Consequently, the savings in memory storage space and computer time is remarkable.

1.2.3 Gwarek Approch

W. K. Gwarek developed the TDFD method for two dimensional problems[11][12]. Consider a structure shown in fig. 2. We take this as a circuit system. The space in which the wave is transmitted is limitted by A and A' in the planes z=0 and z=d. We consider two sets of modes E_n and H_n.

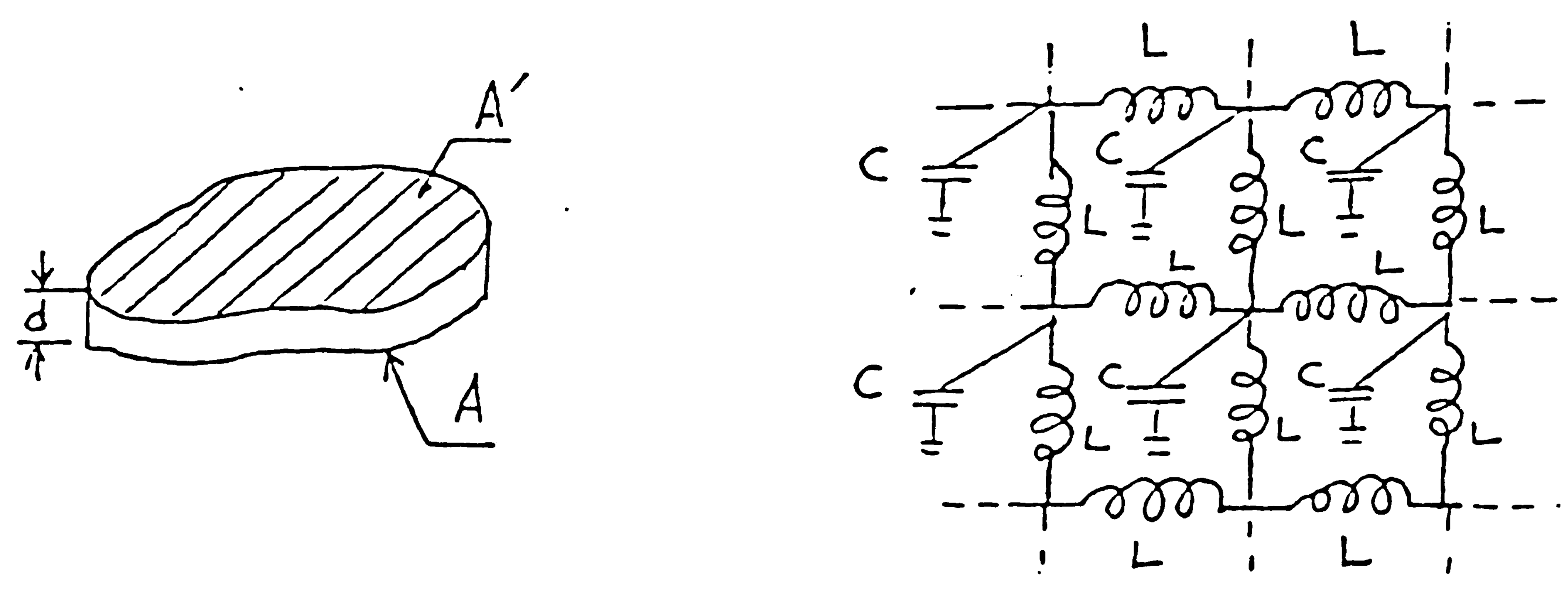

Fig. 2 2-D structure

An E_n mode is a mode described by an electric Hertz potential Π_e of the form

$$\Pi_e^n = a_z \Psi_e^n(x, y) \cos\left(\frac{n\pi}{d} z\right) e^{j\omega t} \qquad (1.7)$$

An H_n mode is a mode described by a magnetic Hertz potential Π_h of the form

$$\Pi_h^n = a_z \Psi_h^n(x, y) \sin\left(\frac{n\pi}{d} z\right) e^{j\omega t} \qquad (1.8)$$

where a_z is a unit vector parallel to z-axis and n is the mode number.

From the general properties of the Hertz potentials we obtain for a electromagnetic field expression $E_n(x,y,z)$ and $H_n(x,y,z)$, where n is a mode number. Based on Hertz potential and EM field quantities, Gwarek gave a definition of surface current J and electrical potential V. The relation between J an V are

$$\nabla \cdot V(x, y) = -j\omega L_s J(x, y) \qquad (1.9)$$

$$\nabla \cdot J(x, y) = -j\omega C_s V(x, y) \qquad (1.10)$$

Consider (1.9) and (1.10) in time -dependent form

$$\nabla V(x, y, t) = - L_s \frac{\partial J(x, y, t)}{\partial t} \tag{1.11}$$

$$\nabla \cdot J(x, y, t) = - C_s \frac{\partial V(x, y, t)}{\partial t} \tag{1.12}$$

the x-y plane is divided into a set of squares of size a. The coordinates of the middle of a mesh in the kth row and lth column are denoted by x_l and y_k. We assume that (1.11) and (1.12) describe propagation of a wave of frequency ω and wavelength λ. If $a \ll \lambda$ and $\Delta t \ll \frac{2\pi}{\omega}$, we may replace the differentials in (1.19) and (1.20) by finite differences Δt and a.

The finite difference equations give a circuit description. The circuit is represented as a set of lumped capacitors C ($= C_s a^2$) and inductors L ($= L_s$) . The potential V has the meaning of the voltage. The current flowing in the inductances may be calculated as $I_x = J_x a$ and $I_y = J_y a$.

1.3 3-D Stripline with Plated Through Hole (PTH) Problem

Investigators used time-domain methods as a tool to deal with simple structure discontinuities . That approach can not meet the design requirements of today's high level of integration package.

A complex but interesting example is a 3-D stripline (not shown in fig. 3) with plated through hole structure. It can be seen very often in multi-layer printed circuit boards. As shown in Fig 3, there are two layers separated by three ground planes with spacing h . There is a microstrip in the middle of each layer with the width W. The strips are connected by a through hole on the middle-ground plane.

Since this is a model that can be applied to many circuit board structures, we take it under study.

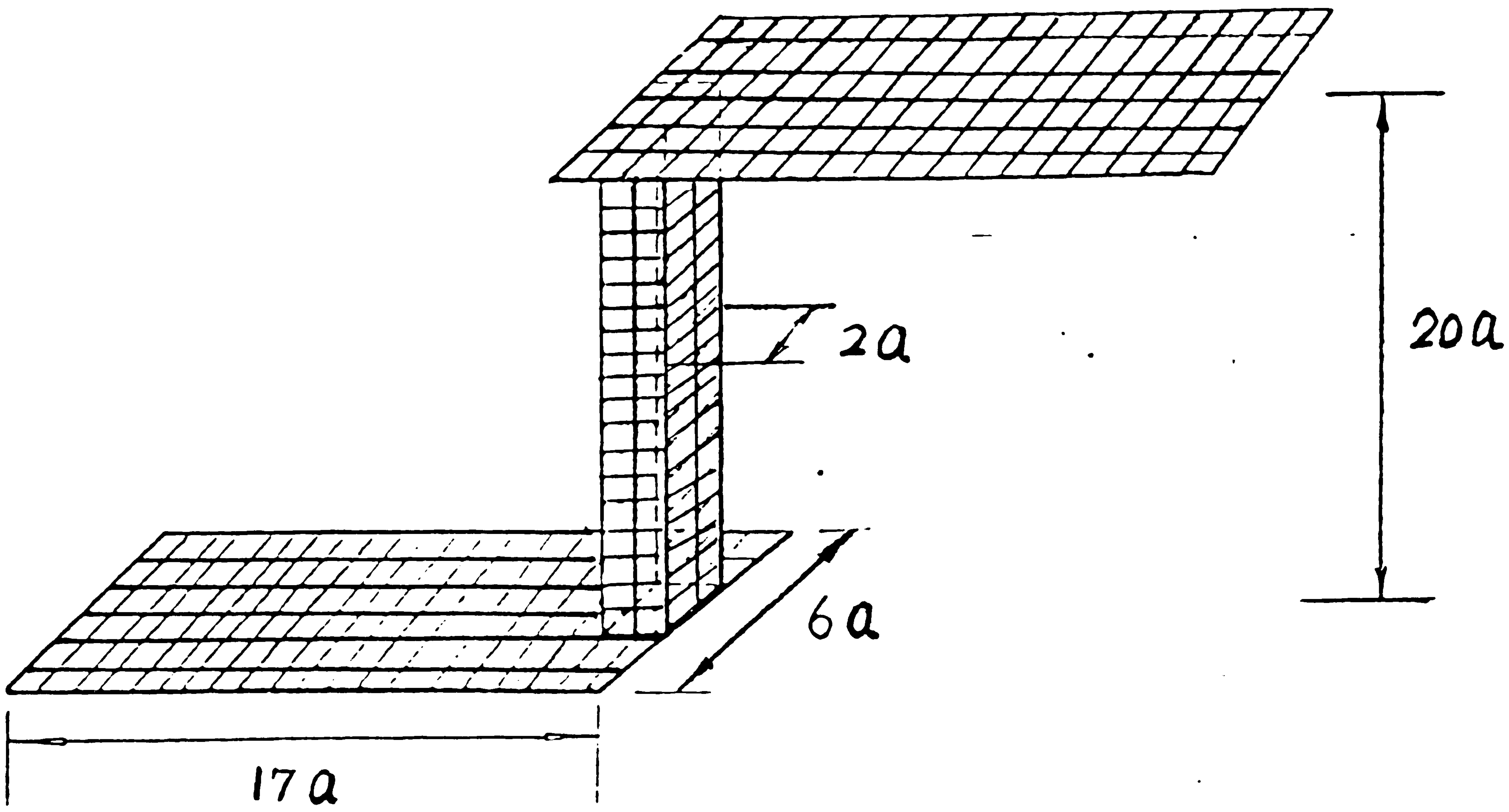

Fig. 3. Stripline with plated through hole (PTH) structure

2. TDFD for Stripline PTH Structure

2.1 General Formulation of the Problem

The generalized 3-D stripline PTH structure under investigation is shown in Fig. 3, where the strip and ground plane are made of a perfect conductor ($\sigma = \infty$) and the substrate has a relative dielectric constant of ϵ_r. The structure is assumed to be in an open environment, that is , above and below the structure , free space is assumed to extend to infinity; in the horizontal direction , apart from the discontinuity region, the layered strip also extends uniformly to infinity.

Assume that current flows on the surface of the structure and the voltage has an instantaneous value on the surface. If we manually unfold the surface into a plane, we get three separated plates, see fig.4 . Here we call the lower strip plate 1, upper strip plate 3, and the via plate 2. Note that we take the strip as an infinitely thin conductor so that there is no change between strip and plate. In practice, the via is a straight circular hole usually. Along the transverse direction the via has a closed surface. When we do the unfolding, we define a cut-line along the hole on the surface so that we can make a plate and keep in mind that this cut-line is only for convenieuce.

After unfolding the structure , we can assume three conducting plates above a ground plane. This assumption can be made since using moment method , we can get capacitance between square segment of plate to ground and inductance on the plates (this can be seen in a later section) .

These circuit parameters give a planar L-C network which looks like connected strip transmission lines.

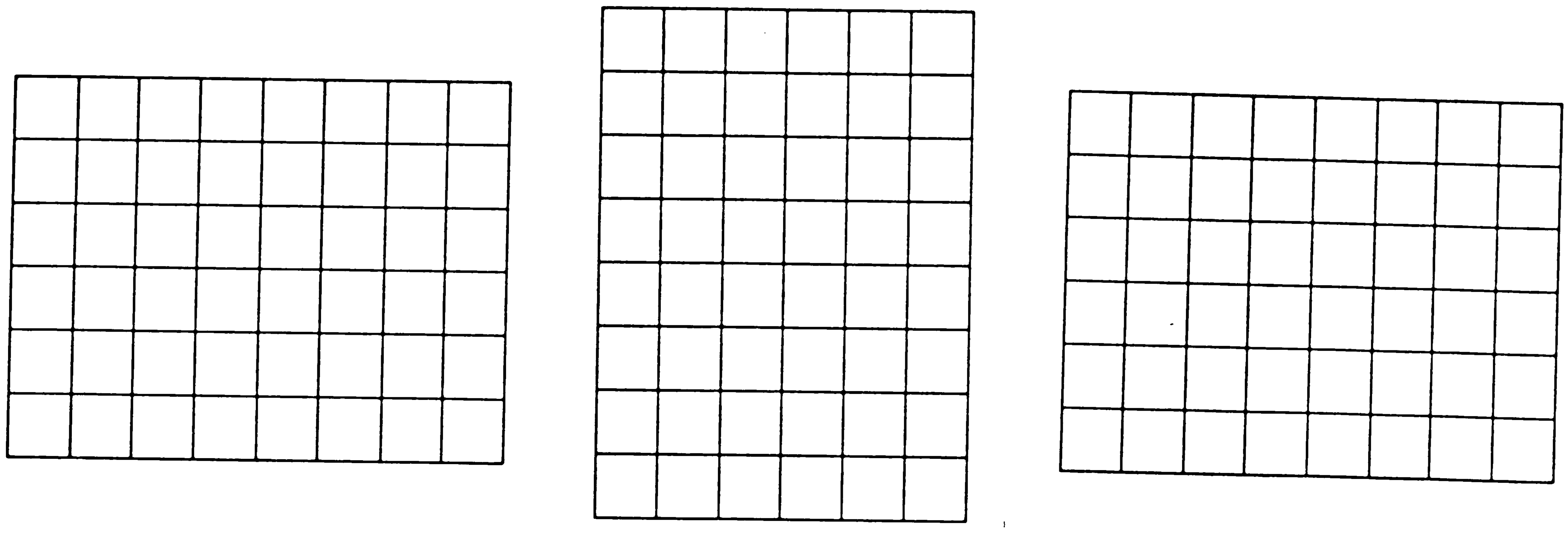

Fig. 4. unfold the PTH surface into three plates

For each plate , the two-dimensional wave equation is obeyed

$$\nabla_{xy}^2 V(x, y, t) - \beta^2 \frac{\partial^2 V(x, y, t)}{\partial t^2} = 0 \qquad (2.1)$$

with proper boundary conditions. In the TDFD method, instead of solving the second-order equation (2.1) a pair of first-order equations is solved:

$$\nabla V_i (x, y, t) = - L_{s\,i} \frac{\partial J_i (x, y, t)}{\partial t} \tag{2.2}$$

$$\nabla \cdot J_i (x, y, t) = -C_{si} \frac{\partial V_i (x, y, t)}{\partial t} \tag{2.3}$$

where i = 1, 2, 3. They refer to plate 1 (lower strip) , plate 2 (via) and plate 3 (upper strip) respectively. At the interface of the three regions, the continuity conditions are enforced. In microwave planar circuits, the variables and constant in (2.2) and (2.3) have the following interpretion: V = voltage, J = surface current density, C_s = capacitance of a unitary square of the circuit, L_s = inductance of an unitary square of the circuit.

For uniqueness of the solution to these equations , the following conditions must be satisfied : a) The initial conditions must be specified on the whole domain of interest; that is V_i (x, y, t=0) and J_i (x, y, t=0) must be given everywhere inside the computation domain. b) The boundary condition of the domain of interest must be given for all t > 0.

2.2 Time Domain Finite Difference Algorithm

The surfaces of the structure are divided into a set of square meshes of size a. Solving equations (2.2) and (2.3) by the finite difference method in consecutive time points simulates the wave propagation. Replacing the differentials in (2.2) and (2.3) by finite differences Δt and a yields

$$J_x\left(x_l+\frac{a}{2},\ y_k,\ t_o+\frac{\Delta t}{2}\right) = J_x\left(x_l+\frac{a}{2},\ y_k,\ t_o-\frac{\Delta t}{2}\right)$$

$$-\left(V(x_l+a,y_k,t_o) - V(x_l,y_k,t_o)\right)\frac{\Delta t}{L_s a} \qquad (2.4)$$

$$J_y\left(x_l,\ y_k+\frac{a}{2},\ t_o+\frac{\Delta t}{2}\right) = J_x\left(x_l,\ y_k+\frac{a}{2},\ t_o-\frac{\Delta t}{2}\right)$$

$$-\left(V(x_l,y_k+a,t_o) - V(x_l,y_k,t_o)\right)\frac{\Delta t}{L_s a} \qquad (2.5)$$

$$V(x_l,y_k,t_o+\Delta t) = V(x_l,y_k,t_o) - \left(J_x\left(x_l+\frac{a}{2},\ y_k,\ t_o+\frac{\Delta t}{2}\right)\right.$$

$$- J_x\left(x_l-\frac{a}{2},\ y_k,\ t_o+\frac{\Delta t}{2}\right) + J_y\left(x_l,\ y_k+\frac{a}{2},\ t_o+\frac{\Delta t}{2}\right)$$

$$\left.- J_x\left(x_l,\ y_k+\frac{a}{2},\ t_o-\frac{\Delta t}{2}\right)\right)\frac{\Delta t}{C_s a} \qquad (2.6)$$

Consecutive calculations of (2.4) , (2.5) and (2.6) simulate the process of wave propagation in the circuit.

2.3 Stability and Convergence

Discrete approximations to partial differential equations are useful only if they are convergent and stable. It is well known that the problem of convergence consists of finding the conditions under which the difference between the theoretical solutions of the differential and the discretized equations at a fixed point (x, t) , tend to zero uniformly, as the net is refined in such a way that a, $\Delta t \rightarrow 0$ and m, n $\rightarrow \infty$, with $m \cdot a$ (= x) and $n \cdot \Delta t$ (= t) remaining fixed. On the other hand , the problem of stability consists of finding a condition under which the difference between the theoretical and numerical solutions of the discretized equation, remains bounded as n tends to infinity.

Lax and Richtmyer have shown [13] that if a linear difference equation is consistent with a properly posed linear initial-value problem, then stability is the necessary and sufficient condition for convergence. Since the problem we are interested in here is a Cauchy type problem and TDFD is a consistent difference approximation to the problem, we only need to examine the conditions under which stability is ensured. There are several ways of analyzing the stability of a hyperbolic system on a regular square grid[15]. Wilson has shown that the leap-frog scheme is stable if

$$c \cdot (\Delta t) \leq a \qquad (2.7)$$

where c is the velocity of propagation. It is interesting to note that this stability criterion is independent of the number of dimensions if the computational grid is uniform, that is , the mesh increment a is the same along any dimension. However for the TDFD scheme the stability condition is found as Courant condition:

$$c \cdot (\Delta t) \leq \frac{a}{\sqrt{n}} \tag{2.8}$$

where n is the number of dimensions.

Boundary conditions and interconnection also can lead to instabilities in the numerical calculation . For the case of hyperbolic systems, the stability question is solved in principle by the theory of Gustafsson, Kreiss, and Sundstrom [14]. Application of this theory is difficult because of its complexity and abstractness. A simple physical interpretation of the main result of this theory was given in terms of group velocity . It is well known that group velocity is a concept associated with energy propagation under dispersive conditions. Its significance to numerical stability results from the fact that finite difference models are necessarily dispersive even on nondispersive equations. This implies that for the numerical approximation, energy associated with different wavenumbers or frequencies will travel at different group velocities, even if the original equation is nondispersive.

Based on this , one can state the main result of the theory of Gustafsson, Kreiss, and Sundstrom as follows. An initial boundary value problem model is stable if and only if

1) the stability condition (2.7 or 2.8) is satisfied everythere inside the mesh boundary;

2) the model (including boundary conditions) admits no wave solutions that grow from each time step to the next by a constant factor z with $| z | > 1$;

3) the model (including boundary conditions) admits no wave solutions with group velocities which support active radiation from the boundary and interconnections conditions to the interior of the computation domain.

2.4 Choice of Excitation

The excitation pulse used in this investigation has been chosen to be Gaussian in shape. A Gaussian pulse has a smooth waveform in time , and its Fourier transform is also a Gaussian pulse centered at zero frequency . These unique properties makes it a perfect choice for this investigation. Also doing computation by TDFD one has to deal with " noise " introduced by discretization of numerical processing which affects the high frequency information. This effect can be minimized if the exciting pulse had the widest possible bandwidth. Such a pulse approaches a delta function and numerically one does it by using a Gaussion pulse.

An ideal Gaussian pulse that will propagate in the + z direction has the following expression:

$$g (t, z) = \exp [- \frac{(t - t_o - \frac{z - z_o}{v})^2}{T^2}] \tag{2.7}$$

where v is the velocity of the pulse in the specific medium, and the pulse has its maximum at $z = z_o$ when $t = t_o$.

The Fourier transform of the above Gaussian pulse has the form

$$G (f) \propto \exp [- \pi^2 T^2 f^2] \tag{2.8}$$

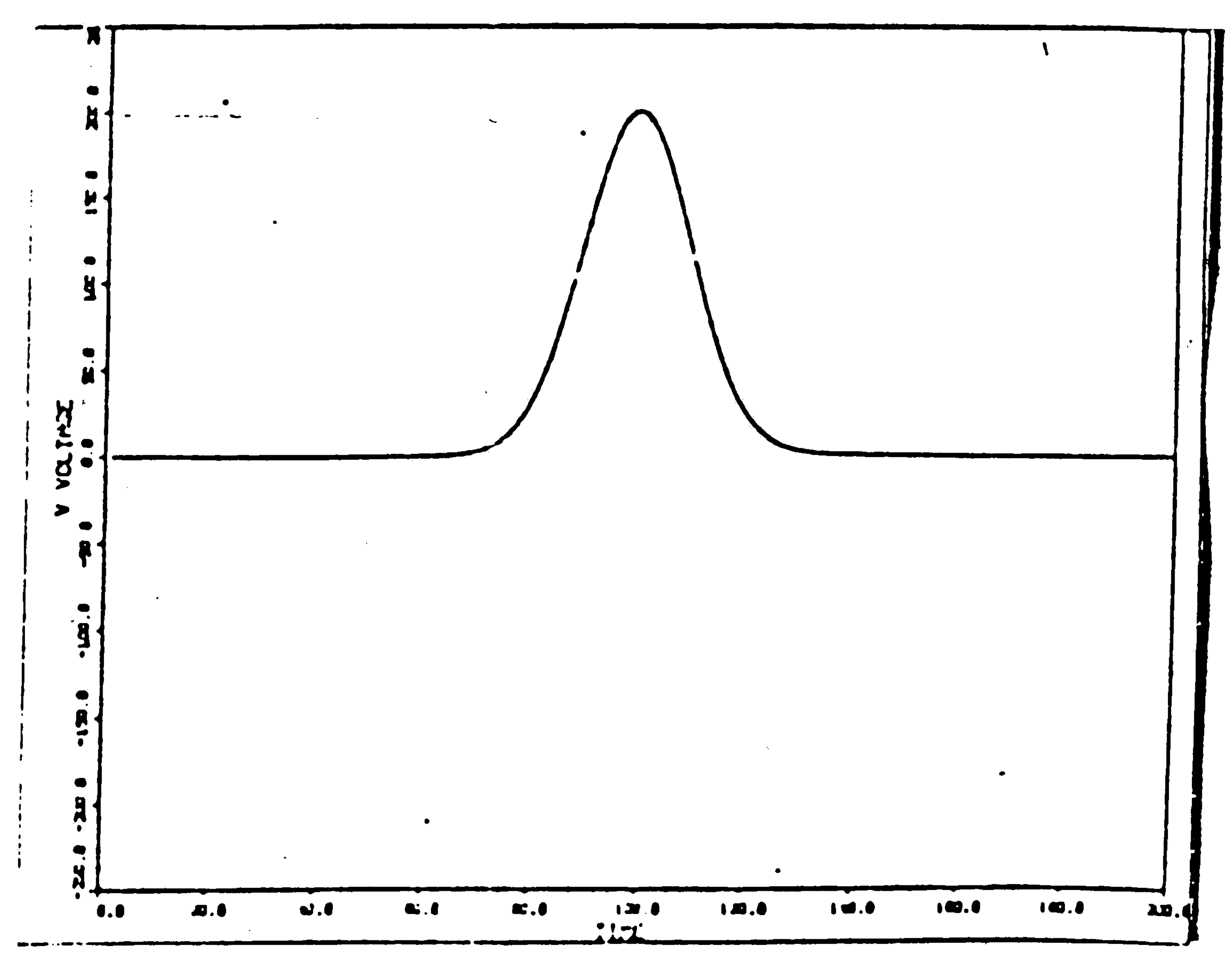

The choice of the parameters T , t_o and z_o are subject to two requirements. The first is that after the space discretization interval Δz has been chosen fine enough to represent the smallest dimenssion of the structure and the time discretization interval Δt has been chosen small enough to meet the stability criterion, the Gaussian pulse must be wide enough to contain enough space divisions for a good solution. And at the same time, the spectrum of the pulse must be wide enough (or the pulse must be narrow enough) to maintain a substantial value within the frequency range of interest. If these two conditions cannot be satisfied simultaneously , Δz has to be rechosen to be even smaller.

The pulse width W chosen in this work is about 60 space step. We define the pulse width to be the width between the two symmetric points which have 5 percent of the maximum value of the pulse. Therefore T is determined from

$$\exp\left[-\frac{(\frac{W}{2})^2}{(vT)^2}\right] = \exp(-3) \simeq 0.05 \qquad (2.9)$$

or

$$T = \frac{10\ \Delta z}{\sqrt{3}\ v} \qquad (2.10)$$

By making this choice of T , the maximum frequency which can be calculated is

$$f_{max} = \frac{1}{2T} = \frac{\sqrt{3}\ v}{20\ \Delta z} \quad (2.11)$$

with the specific Δz chosen , it is high enough to cover the entire frequency range of interest.

The second requirement is that the choice of z_o and t_o be made such that initial " turn on " of the excitation will be small and smooth.

2.5 Matching Boundary Conditions

The TDFD method models the energy flow in the circuit . If the input and out put of the circuit are matched , energy flow can be well represented and we can use it to compute the S matrix and other frequency domain data directly.

Consider the input and output ends of the PTH structure, Fig. 6. the width $w = 6\ a$ where a is the mesh size. Input and output matching is obtained by introducing in each of the rows of meshes at the input and output the following operations:

$$I_1(t_0 + \frac{\Delta t}{2}) = I_1(t_0 - \frac{\Delta t}{2}) - (V_2 (t_0) - V_1 (t_0)) \frac{\Delta t}{L} \quad (2.12)$$

$$V_1(t_0 + \Delta t) = V_0(t_0 + \Delta t) - I_1 (t_0 + \frac{\Delta t}{2}) R_0 \quad (2.13)$$

$$I_{n+1}\left(t_0 + \frac{\Delta t}{2}\right) = I_{n+1}\left(t_0 - \frac{\Delta t}{2}\right) + \left(V_{n+1}(t_0) - V_{n+2}(t_0)\right)\frac{\Delta t}{L} \qquad (2.14)$$

$$V_{n+2}(t_0 + \Delta t) = I_{n+1}\left(t_0 + \frac{\Delta t}{2}\right) R_0 \qquad (2.15)$$

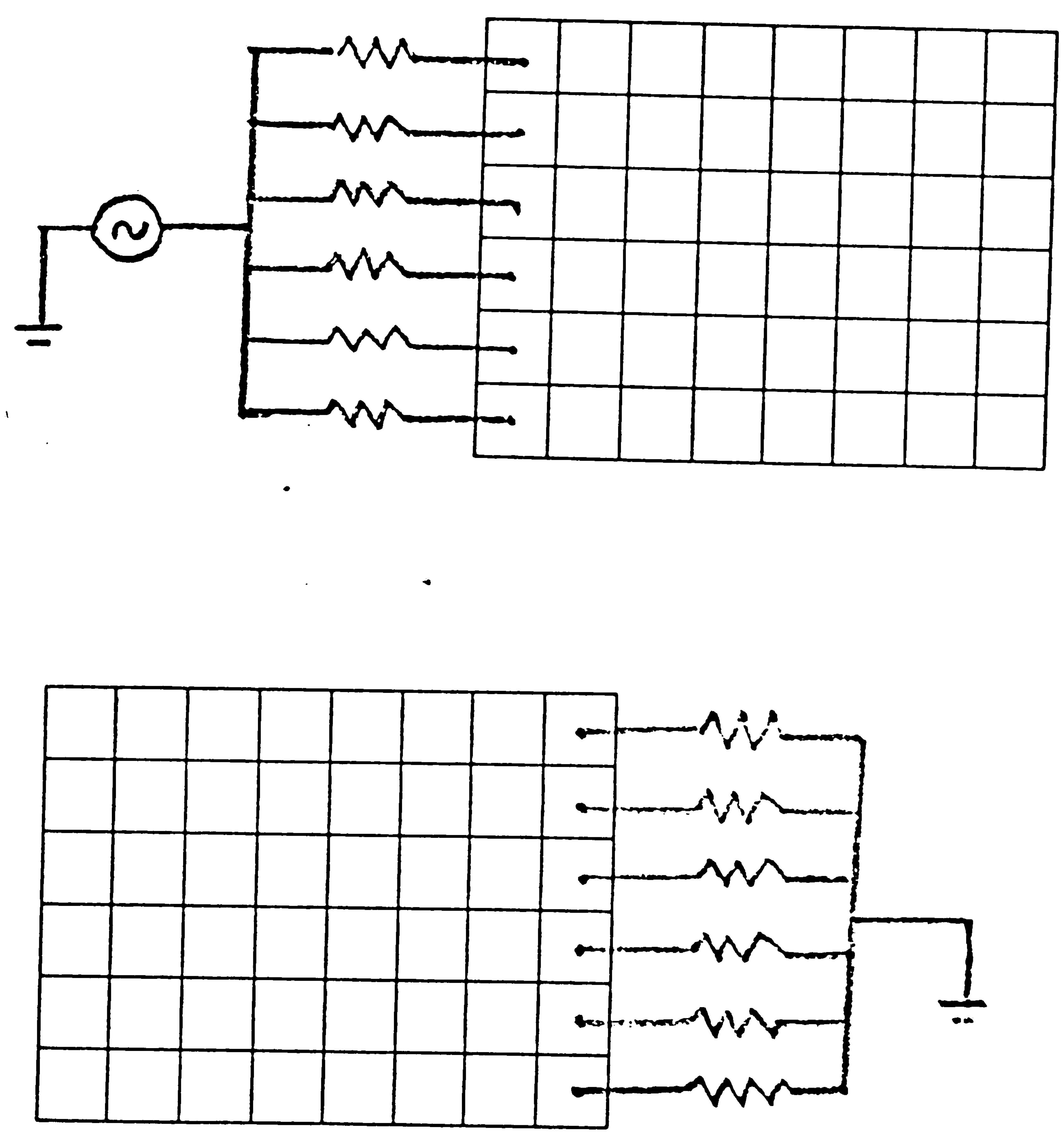

Fig. 6 Matching boundary conditions

2.6 Interconnection Conditions

Since we artificially decompose the problem into three plates, interconnection between the plates should be arranged properly based on the real structure. For each segment we use a central node for voltage sampling. Also along the edge we connect to branches for current sampling in x and y directions. It is clear that at the interconnection region, the current must be continuous. Base on this fact , we have interconnection shown in fig. 6.

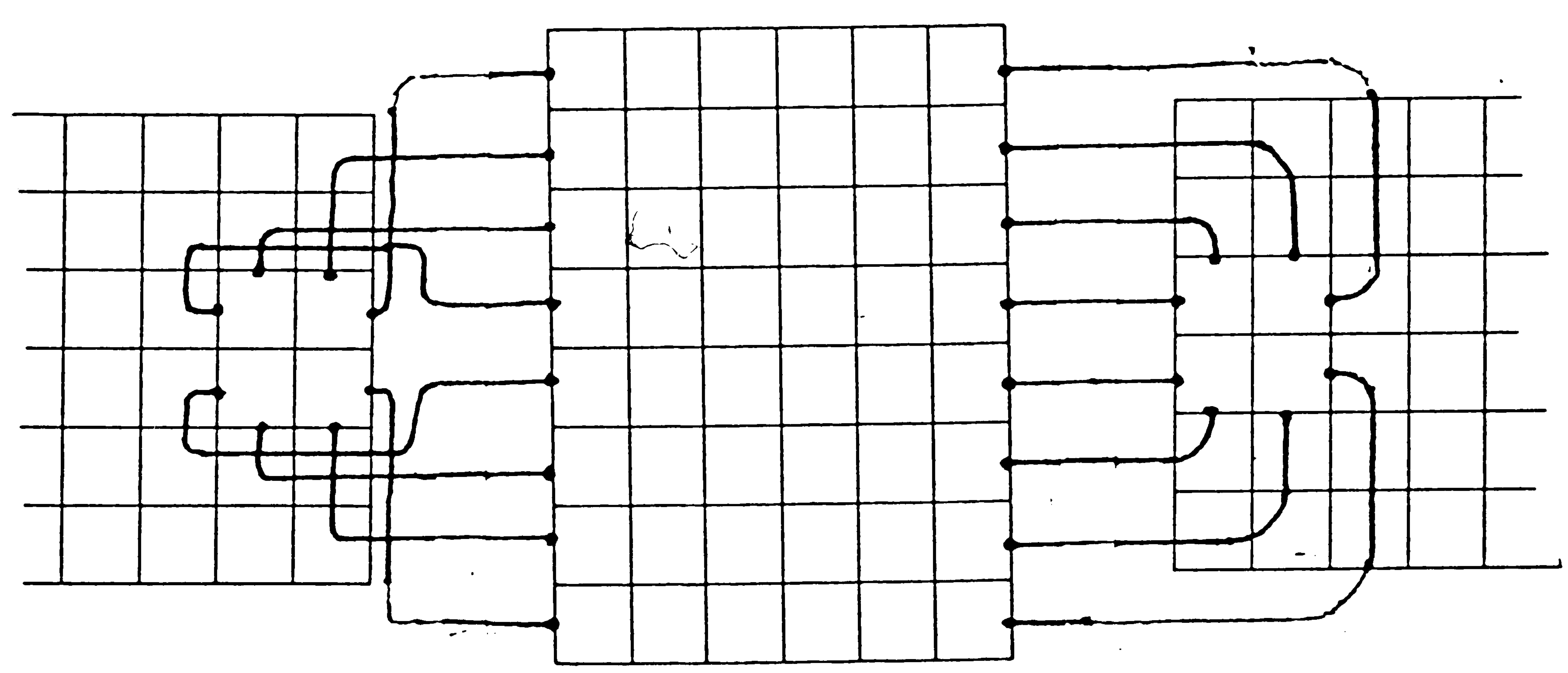

Fig. 7. Interconnection between the plates

2.7 Capacitance and Inductance Calculation

Gwarek calculated capacitance and inductance based on equations 1.15–1.18 . This approach gives a uniform distribution of capacitance and inductance which is not true in the real world. The fringing field must be considered even for a single strip case. The stripline PTH structure has two layers separated by three ground planes with a hole in the middle that connects to the signal lines . The complexity of the structure requires us to take into account the friging field more carefully.

Ed Li and Professor Decker developed a technique to calculate the capacitance and inductance matrix by the Method of Moments combined with structure symmetry considerations. This technique considers all the edge effect coupling. The results obtained show a reasonable distribution of capacitance and inductance on the strips . We use these data for the TDFD calculations.

3 NUMERICAL RESULTS

The Transient analysis for the stripline PTH structure has been performed by the method described in preceding section. In Fig.3 the model of the stripline PTH structure is shown. The parameters of the structure are shown as follows:

width of the strip W_s = 0.2 mm

length of the strip L_s = 0.561 mm

width of via W_v = 0.24 mm

length of via L_v = 0.6 mm

To accommodate the structural details of the strip, the mesh parameters have been chosen to be

space interval for strip : $a = 0.0333$ mm ($\Delta x = \Delta y = a$)

space interval for via : $a_v = 0.03$ mm

time step $\Delta t = k \cdot a/c$ (sec) , where c is the velocity of light in air and k is a constant restricted by the stability criterion.

A Gaussian pulse excitation is used at the input side. It is uniform across the strip and has the following specified value:

$$V(t) = \exp\left[- \frac{(t - t_0)^2}{T^2} \right]$$

where $t_0 = 100\ \Delta t$ and $T = 10\ \Delta t$. The frequency spectrum of this pulse is from DC to about 100 GHz.

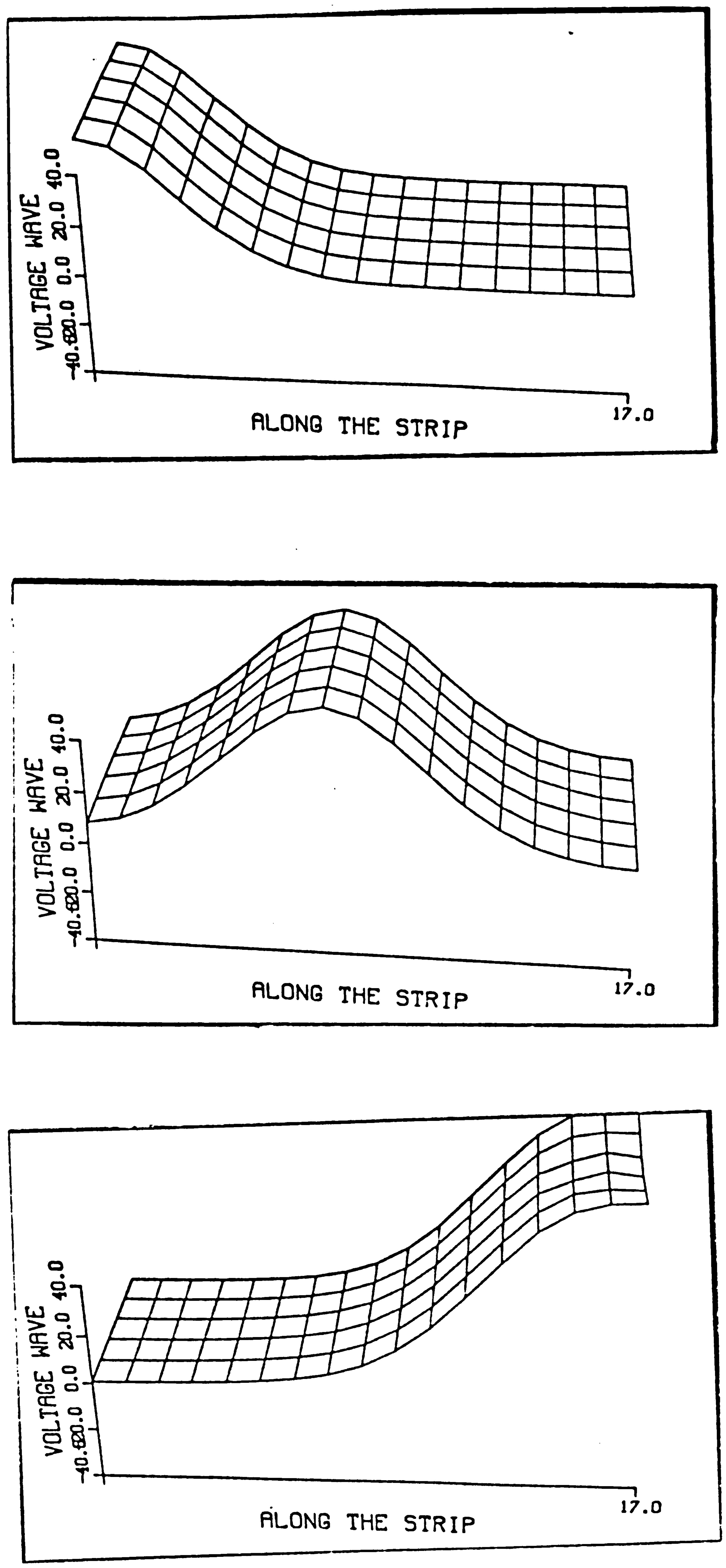

Fig. 9 . Voltage distribution on stripline 1

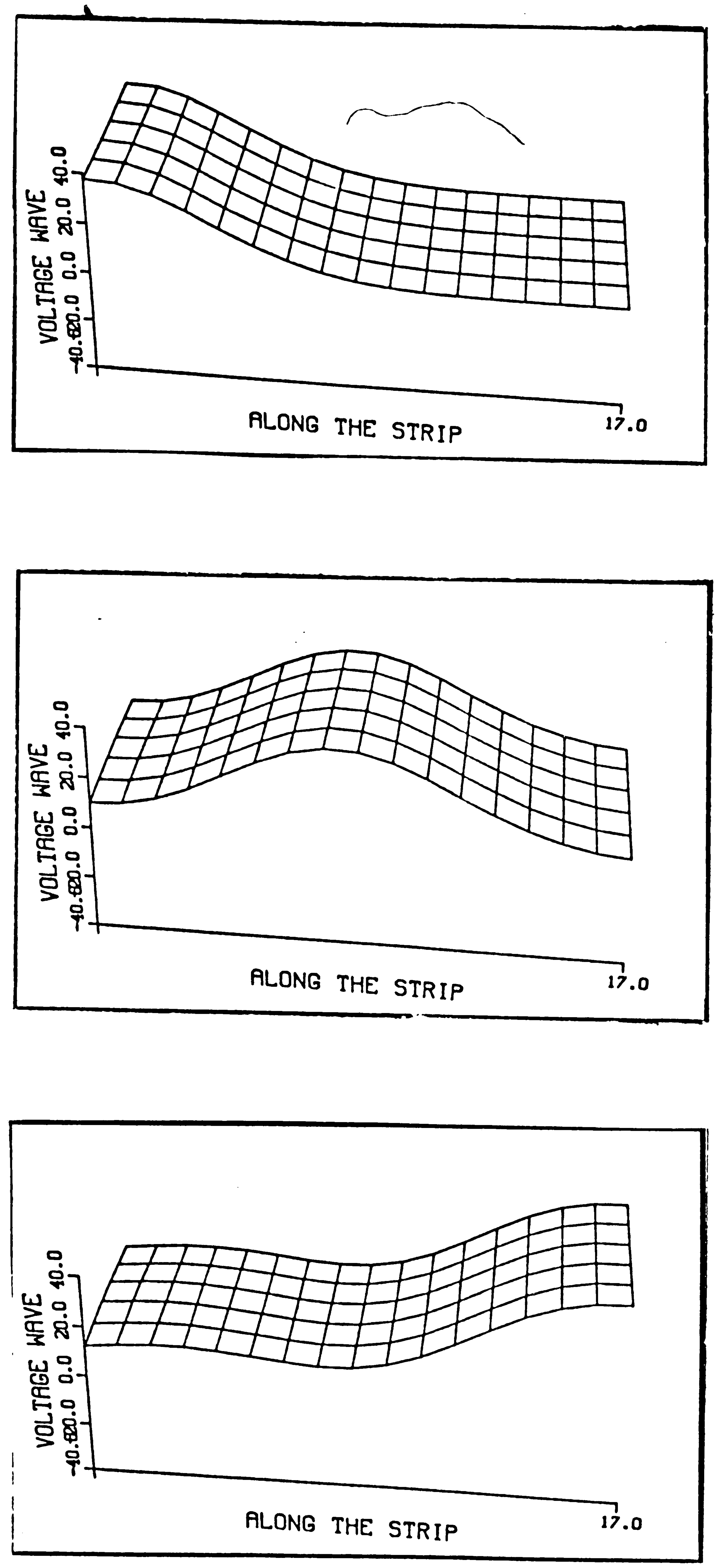

Fig. 10 . Voltage distribution on stripline 2

Fig. 8 (a) shows the calculated voltage wave along the strip at $t = 200\ \Delta t$. At this time a gauss pulse reaches the matched input port. The rest of stripline has not get any excitation so that it remains quiet. Fig. 8 (b) shows the voltage distribution at $t = 250\ \Delta t$. We can see that the wave propagates along the strip 1 with constant velocity and no loss (the strip is a perfect conductor) . When the wave reaches the hole fig. 8(c) $t=300\Delta t$, potential along the transversal direction is built because of the capacitance distribution in this region.

When the wave passes through the hole , Strong reflection occurs, and transversal mode is generated because that the hole is excited non-uniformly.

Fig. 9 (a) shows the wave reaches the second strip at $t=450\Delta t$. At this time, voltage amplitude becomes lower because the loss at mismatched interconnection condition. After a while , potential distribution along the transversal direction becomses uniform and wave propagates with constant velocity again shown in fig. 9 (b) $t=500\Delta t$. At $t= 550\Delta t$, the wave reaches output port as shown in fig. 9 (c). We can see that the wave changes its shape because the reflection generates noise at the interconnection region.

The program is in C Language. It take 4 minites to run 600 time step in a HP computer. Instant voltage display can be seen on the screen and selected data can be found in a data file for further study.

3. SUMMARY AND FUTURE RESEARCH

The TDFD algorithm has several advantages over other schemes for the calculation of microstrip time-domain fields. It uses Maxwell's equations directly . Therefore it has clear physical interpretation. If a computional error occurs, its cause can be quite easily spotted. It simulates the wave propagation in the circuit numerically. The central difference nature of the leapfrog method makes it a relatively accurate method (second order accuracy in both time and space), compared to other first order schemes . The leapfrog algrithm has the unique characteristics that the numerical scheme has no dissipation (amplitude increase or decrease for any frequency component) and only a small amount of dispersion. It has been shown that the numerical dispersion is negligible compared to the physical dispersion of the strip.

The paper has presented a version of the finite-difference time-domain method for transient calculation of 3-D stripline PTH structures. Only theoretical and numerical work is done at this stage. We need experimental data (such as S parameters mesured by network analyser) to verify our result. In order to do this , Fourier transform needed to get frequency domain data and S parameters.

References

[1] G. Kompa and R. Mehran , " Planar waveguide model for calculating microstrip components," Electron.lett., vol. 11, pp. 459-460, Dept. 1975

[2] W. Menzel and I.Wolff," A method for calculating the frequency dependent properties of microstrip discontinuities," IEEE Trans. Microwave Theory Tech., vol MTT-25, pp.107-112, Feb. 1977.

[3] J. R. James and A. Henderson, " High-frequency behavior of microstrip open-circuit terminations," IEE J. Microwave Opt. Acoust., vol. 3, pp. 205-211, Sept. 1979.

[4] R. H. Jansen, "The spectral-domain approach for microwave integrated circuits," IEEE Trans. Microwave Theory Tech., vol MTT-33, pp.1043-1056, Oct. 1985.

[5] P. B. Katehi and N. G. Alexopoulos, "Frequency-dependent characteristics of microstrip discontinuities in millimeter-wave integrated circuit," IEEE Trans. Microwave Theory Tech., vol MTT-33, pp.1029-1035, Oct. 1985.

[6] R. W. Jackson and D. M. Pozar," Full-wave analysis of microstrip open-ended and gap discontinuities," IEEE Trans. Microwave Theory Tech., vol MTT-33, pp.1036-1042, Oct. 1985.

[7] X. Zhang, J. Fang, K.K. Mei, and Y. liu, " Calculation of the dispersive characteristics of microstrips by the time-domain finite difference method," IEEE Trans. Microwave Theory Tech., vol. MTT-36 pp. 263-267, Feb. 1988 .

[8] K. S. Yee, " Numerical solution of initial boundary value problems involving Maxwell's equations in istropic media ," IEEE Trans. Antennas Propagt., vol. AP-14, pp. 302-307, May 1966

[9] X. Zhang and K.K. Mei, " Time domain finite difference approach for the calculation of microstrip open circuit end effect," 1988 IEEE MTT-S Digest , pp 363-366

[10] N. Yoshida, I. Fukai,"Transient analysis of a stripline having a corner in three-dimensional space," IEEE Trans. Microwave Theory Tech., vol. MTT-32 pp. 491-498, May. 1984.

[11] G. Metzger and J-P. Vabre, Transmission lines with Pulse Excitation. New York: Acadmic Press, 1969, pp 65-96.

[12] W. K. Gwarek, " Analysis of an arbitrarily-shaped planar circuit – A time domain approach," IEEE Trans. Microwave Theory Tech., vol. MTT-33 pp. 1067-1072, Oct. 1985.

[13] W. K. Gwarek,"Analysis of arbitrarily shaped two dimensional microwave circuits by finitr difference time domain method," IEEE Trans. Microwave Theory Tech., vol. MTT-36 pp. 738-744, April 1988.

[14] P. D. Lax and R. D. Richtmyer, " Survey of the stability of linear finite difference equations, " J. Inst.Math. appl., vol. IX , pp. 267-293, 1956

[15] A. R. Mitchell and D. F. Griffiths, The Finite Difference Method in Partial Differential Equations. New York: Wiley, 1979

[16] B. Gustafsson, H. O. Kreiss, and Sundstrom, " Stability theory of difference approximations for mixed initial boundary value problems II , "

Maths. Comp., vol. 26, pp 649-686, 1972.

[17] P. B. Johns, " On the relationship between TLM and finite-difference methods for Maxwell's equations, " IEEE Trans. Microwave Theory Tech., vol MTT- 35, pp. 60-61, Jan. 1987.

[18] D. T. Borup, D. M. Sullivan, and O. P. Gandhi, " Comparison of the FFT conjugate gradient method and the finite-difference time-domain method for the 2-D absorbtion problem," IEEE Trans. Microwave Theory Tech., vol MTT- 35, pp. 383-395, Apr. 1987.

[19] A. Taflove and M.E. Brodwin, " Numerical solution of initial stady-state electromagnetic scattering problems using the time-dependent Maxwell's equations," IEEE Trans. Microwave Theory Tech., vol MTT-23, pp. 623-630, 1975.

[20] S. Koike, N. Yoshida, and I. Fukai, " Transient analysis of microstrip gap in three-dimensional space," IEEE Trans. Microwave Theory Tech., vol MTT- 33, pp. 726-730, Aug. 1985.

[21] S. Koike, N. Yoshida, and I. Fukai, " Transient analysis of coupling between crossing lines in three-dimenssional space," IEEE Trans. Microwave Theory Tech., vol MTT- 35, pp. 67-71, Jan. 1987.

[22] K. S. Knuz and K. M. Lee , " A three-dimensional finite-difference solution of the external response of an aircraft to a complex transient EM environment : Part I – The method and its implementation, " IEEE Trans. Electromangn. Compat., vol EMC- 20, pp. 328-333, May 1978.

[23] A. Taflove, " Application of the finite-difference time-domain method to sinusoidal steady-state electromagnetic-penetration problems," IEEE

Trans. Electromangn. Compat., vol EMC- 22, pp. 191-203, Aug. 1980.

[24] K. K. Mei, A. Cangellaris, and D. J. Angelakos, " Conformal time domain finite difference method, " Radio Sci., vol. 19, pp 1145-1147, Sept.-Oct. 1984.

[25] A.Farrar and A.T. Adams, " Matrix method for microstrip three-dimensional problem," IEEE Trans. Microwave Theory Tech., vol MTT-20, pp.497-504, Aug. 1972.

Vita

Zhigang Ma graduated from Beijing University of Posts And Telecommunications with a Bachelor of Science Degree in Electrical Engineering in 1981. As a visiting scholar , he spent one year doing research of electromagnetic field-to-wire coupling in the SHF/EHF frequncy range at Syracuse University. He is currently pursuing a Master of Science Degree in Electrical Engineering at Lehigh University .